# A Study on Dynamic Behaviours of Electron Beam Welding (Report I)†
## —The Observation by a Fluoroscopic Method—

Yoshiaki ARATA,* Eiichi ABE** and Masanao FUJISAWA **

**Abstract**

*An experimental technique utilizing a cine-fluoroscopy and a metal tracer was developed to continually monitor the electron beam welding process. This technique made it possible to observe the dynamic nature of the beam hole more directly and more clearly than some others.*

*Using aluminum alloys as the parent metal, some phenomena related to the beam-metal interactions such as the big wall-fluctuation at the back side of the beam hole ("wall-cave" and "wall-knob"), the formation of root porosity due to the arched curvature of the beam hole, the behaviours of spiking concerned with the hole shape, and in part the rapid movement of the molten metal were apparently revealed.*

## 1. Introduction

It has been suggested that a vapor filled capillary is formed in the path of an electron beam[1,2] and is rapidly filled with molten metal as electron beam welding progresses. The term "beam hole" is here adopted to indicate such a capillary which has been called a (weld) cavity or (penetration) channel and so on.

Little is known, however, about the actual mechanism which determines the size and the shape of the beam hole and their time development during welding, because of many difficulties lying on the technique to observe directly those dynamic behaviours, while some works were attempted utilizing elavorate equipments. Tong and Giedt[1] first used radiography of pulsed X-ray for such investigation. However, since they could only take single pictures of which the definition and resolution were still unsatisfactory to reproduce, it was impossible to acquire continually an overall impression of the very rapid processes. Funk, McMaster et al.[2] employed a pinhole streak camera and recorded the X-ray intensity distribution which was emitted from the beam hole. While they could roughly reveal the time related position and intensity of electron beam impingement, dynamic behavior of beam hole and molten pool could not be observed on their high speed pictures. For this reason, a trial was initiated in which a fluoroscopic technique was used for continuous observation of the phenomena.

## 2. Experimental Method

### 2.1 System for observation and recording

The experimental arrangement of the equipment is shown in Fig. 1. The X-rays emitted from the X-ray source pass through a work piece during actual welding, and impinge onto an X-ray image intensifier in which they are collimated and amplified being converted into light-rays and electrons. Finally, the visible images are obtained on the second fluoresent screen and they are filmed with a movie camera.

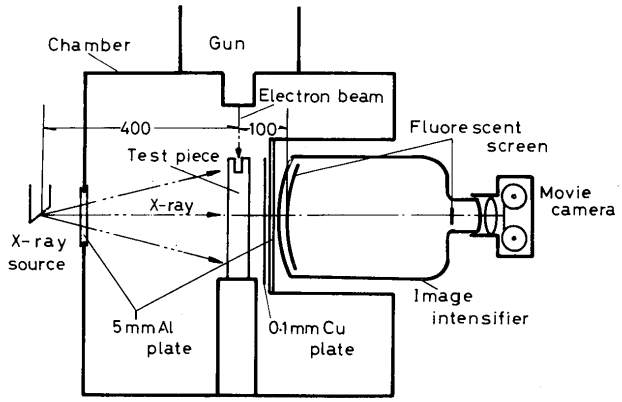


Fig. 1 Schematic figure of experimental technique

In electron beam welding, the welder itself works as an X-ray generator and X-ray is emitted from the wall of the beam hole produced by welding electron beam. So

† Received on Jan. 14, 1976
* Professor
** The Tokyo Metropolitan Research Institute of Industrial Technology

such X-ray is here called "beam hole X-ray." The resolution and contrast of the image on the fluorescent screen are reduced by the incidence of the beam hole X-ray and the other scattering X-ray. Thus a mask of copper plate 0.2 mm thick was provided upon the input window of the image intensifier to absorb these disturbing X-ray. The decrease of discernability caused by the copper plate was only 0.5% in the penetrameter sensitivity (that is the indication of radiographic resolution). In order to obtain a good image quality, it is important to set up suitable distances between the X-ray source, the welding zone to be detected and the image intensifier. The image intensifier should be set as close as possible to the welding zone for preventing the decrease of picture definition due to the enlargement. For the same reason, the smaller focal spot of the X-ray tube is, the better definition and resolution are gained on the picture. So, in this experiment, a d.c. X-ray equipment Müller MG 150 was employed as the X-ray source with its focal spot of 0.7 mm x 0,7 mm and Philips image intensifier tube MB 13 (diameter 6 inches) was located at the bored vacuum chamber as illustrated. Being aligned the center axis, a 16 mm cine camera was placed behind the viewing screen of the tube. The films used were Fuji type RKS-FG for fluoroscopic use. The input and output side windows of the vacuum chamber were both constructed of 5 mm thick aluminium plate instead of steel to decrease X-ray absorption.

For a given X-ray spectrum and intensity, the resolution and contrast of the image also depend to a great extent on the thickness ratio of X-ray penetration between the beam hole to be detected and the material to be welded. Hence a given void size can be most easily detected in thin specimens. But in thin specimens, the depth of weld penetration is severely limited since the specimens are apt to be over heated with a low power of electron beam, and show some behaviours different from the ordinary welding. Compromise specimen thickness of 12–20 mm was chosen in this experiment.

## 2.2 Experimental Procedure

Experiments were composed of two serieses of welding runs. In the first series, aluminum alloy 5083 (4.6Mg, 0.01Zn, 0.02Ti, 0.15Cr, 0.04Cu, 0.21Fe, 0.64Mn, 0.14Si, Bal, Al) was used as the parent metal and silver brazing alloy (75Ag-25Cu) was inserted as the tracer.

Without any tracers, the fluoroscopic images would yield no informations about the extent and the flow motion of the molten metal since the density difference between melt and solid is very slight. To discern the movement of the melt at least in part, a material which had higher absorption coefficient than the parent metal had to be employed as a tracer.

The size and shape of the specimens and the position of inserted tracers were illustrated in Fig. 2, and the conditions of welding and X-ray irradiation were as shown in Table 1. The lens current of 0.82 amperes made the

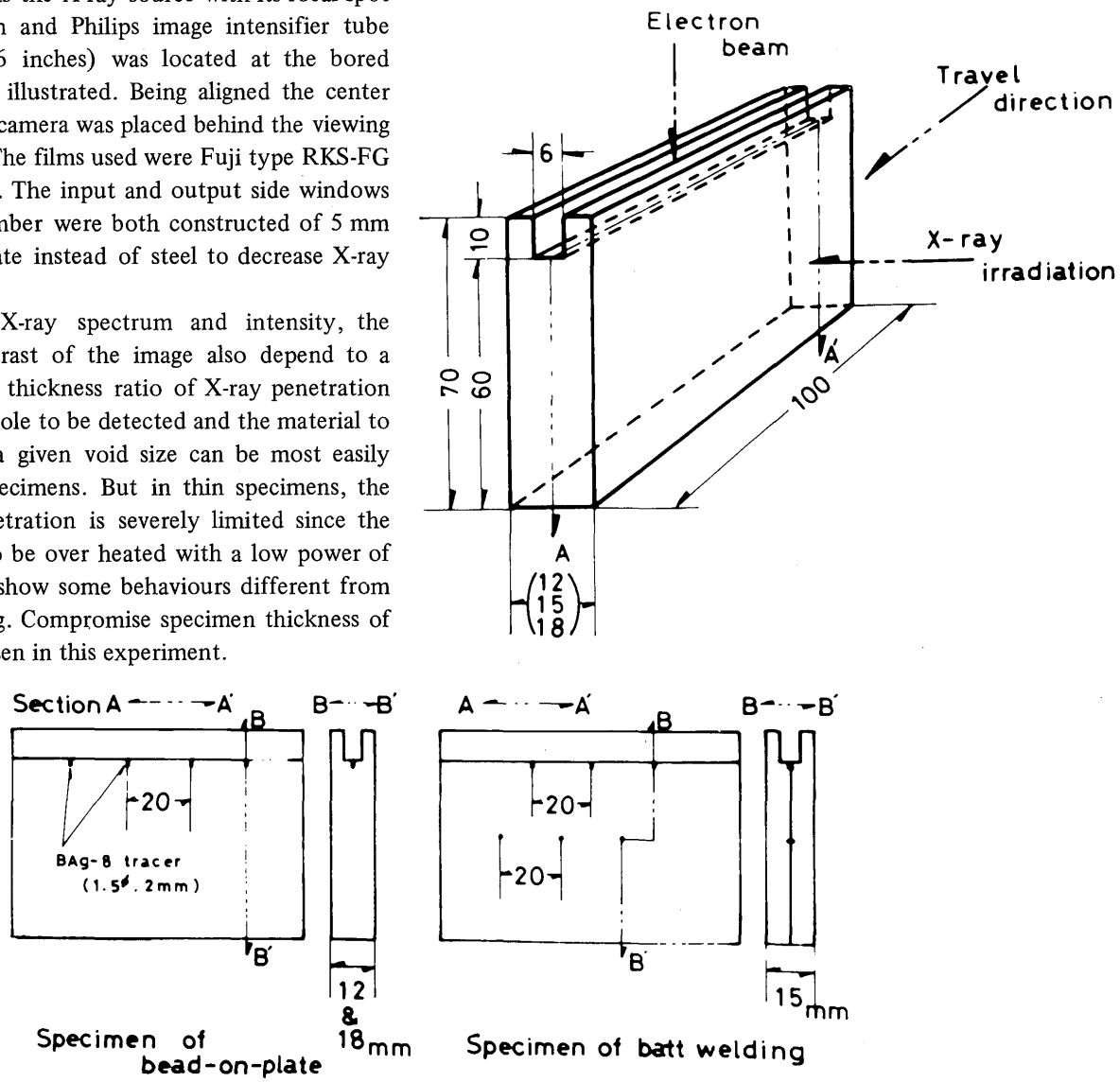


Fig. 2 Test specimen and position of inserted tracers (Series. 1)

focal point just on the surface of specimen ($a_f$ value = 1). The weld penetrations reached into about 50 mm in these conditions.

Table 1 Experimental condition (Series 1)

| Welding Condition | | | Width of plate | X-ray irradiation (Focal spot 0.7 x 0.7 mm) | | |
|---|---|---|---|---|---|---|
| Fixed factors | Lens current (A) | Process | | Tube volage | – | Tube current |
| 30kV | 0.82 | Bead-on -plate | 12mm | 60kV | – | 8mA |
| 250mA | 0.84 | | | | | |
| 75mm (W.D.) | 0.82 | Butt weling | 15mm | 63kV | – | 8mA |
| 300mm/min | 0.84 | | | | | |
| | 0.82 | Bead-on -plate | 18mm | 65kV | – | 8mA |
| $2 \times 10^{-5}$ Torr | 0.84 | | | | | |

* Note; W.D. = work distance

At the bottom part of the beam hole, the size of the void becomes smaller than at the upper part. The resolution of the film decreases to make it difficult to discern the shape of the hole.

In the second series, in order to improve the discernabity, copper foils were inserted at the lower part of the specimen. It was considered to be important to observe the bottom part more clearly since the spiking, which is one of the inherent defects in partial penetration electron beam welding, appeared at the part. By changing the inserted metal from pure copper to brass and also by changing its location, the effect of highly volatile element on the shape of beam hole and also on the formation of spiking was examined.

The location of inserted metal and the size of specimens were illustrated in Fig. 3, and in this series a grid made of stainless steel wire was located at the front of the first fluorescent screen to indicate the demensions. One spacing of this grid was about 8 millimeters on the obtained films. The welding conditions were as shown in Table 2.

Table 2 Welding condition (Series 2)

| Film | Material (width mm) | Welding speed cm/min | Work distance mm | Lens current* Amp. | Inserted Metal (0.2t) |
|---|---|---|---|---|---|
| No. 4 | 5083 Alloy (20) | 30 | 65 | 0.84 | Copper |
| No. 5 | | 50 | 40 | 0.95 | Brass |
| No. 6 | Aluminum A1100(20) | 50 | 40 | 0.965 | Copper |
| No. 7 | | 50 | 40 | 0.965 | Brass * |

Location of inserted foils are at the lower part and (*) at the upper part. (Specimens are butt welded)

Experiments were conducted with a low voltage type welding unit which had the maximum capacity of 7.5 KW at 30 KV (and 15 KW at 60 KV).

The chamber was evacuated, welding parameters and X-ray irradiation parameters were set, and sequentially, the camera motor was started, and a little later, the welding operation was initiated. The film was moved at a framing rate of about 50 per second.

## 3. Experimental Results and Discussions

### 3.1 Quality of obtained films.

The data was obtained in the form of exposed films which were several meters in length.

The contrast of the original film was rather low, but it could be risen to a certain extent by means of reprinting the original on a reversal film. As for the resolution, wires in the penetrameter which had a diameter of more than 0.8 mm were clearly visible on the viewing screen of image intensifier, but on the frames of the film, the minimum

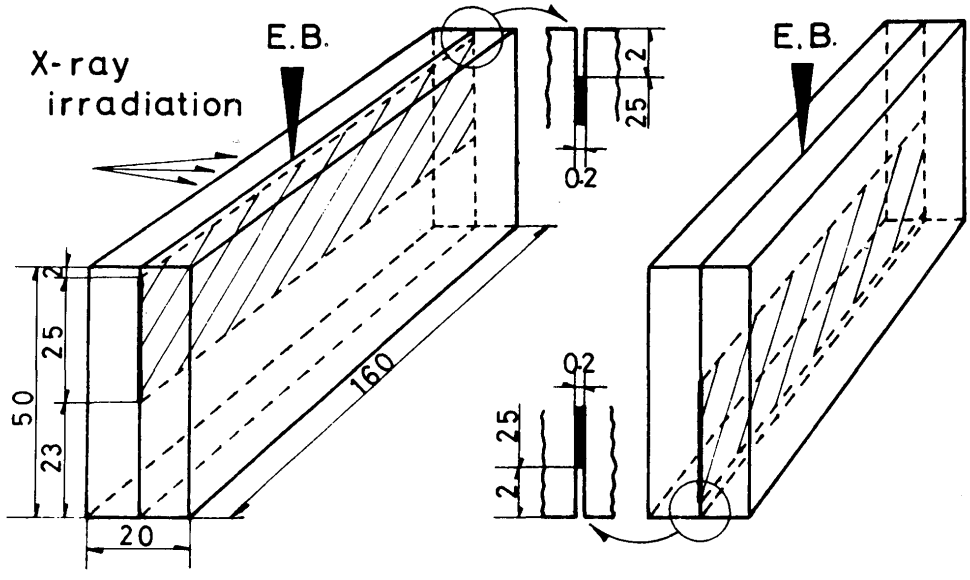


(a) Inserted at the upper part (b) Inserted at the lower part

Fig. 3 Dimension of specimens and position of inserted foils (Series 2)

diameter of discernable beam hole was to be believed about 1 mm. A reasonable first approach to get a better resolution would be to select the material of the chamber windows such as beryllium which has a less X-ray absorption ability than aluminium employed in practice. It is not preferable to use thinner specimens for welding since the natural behaviours of the process may be distruved in return for decreasing the total thickness of the materials through which X-ray must penetrate.

In the second series of welding runs, the resolution and contrast of the film increased at the part where copper or brass foils was inserted.

### 3.2 Influence of inserted metals on the natural bahaviours of beam hole and molten metal

As for the selection of added tracers and inserted foils, each of these materials should have a larger atomic number than aluminium, the parent metal, from the view point of X-ray absorption. On the other hand, such a material has a higher specific gravity, and there is the possibility that they sink or sediment at the bottom of the moten pool.

The tracers which have a better affinity for the parent metal are expected to flow together with the molten metal giving less effect upon its natural movement. Therefore, a silver brazing alloy was considered to be preferable because its melting point is not so far from that of aluminium, and silver has a good solubility for aluminium, beside it was commonly available as a form of wire rod.

In spite of the high vapor pressure of silver, no remarkable change was recognized in the shape of beam hole even at the very place where the tracer was inserted. It might account for this that as concerned with the vapor pressure silver is higher than aluminium but lower than magnesium which is involved in 5083 alloy. Consequently, it was supposed that the behaviours of the molten pool or beam hole were not affected so much by the addition of the small amount of such tracers. (Photo. 2)

As copper foils are concerned, the problem of the vapor pressure can be neglected since they have the lower one than aluminium. But the difference of the penetration depth or the spiking phenomenon between the weld with and without the copper foil was not yet examined, so the influence of inserted copper was remained as a problem for a further investigation.

### 3.3 Behaviours of the beam hole

Observing these films, it is immediately apparent that, as the welding is initiated, the formation of the beam hole begins with vaporizing the material along the path of electron beam. The beam hole increases its depth until an equilibrium is established, and then a nearly constant depth is continually produced for the duration of welding. While the beam hole varies its size and shape with the time, and shows a oscillatory nature.

In the first series, the cyclic wall-fluctuation of beam hole happened very rapidly and developed upward. In this case the strong wall-fluctuation gave rise to the big cave and knob at the wall. The terms "wall-cave" and "wall-knob" are here adopted to indicate such caved part in and swelled part on the wall respectively. Such wall-caves, which seemed the local expansion of gas bubbles due to the high pressure of the evaporating metal, were observed in the beam hole. These wall-caves grew up gradually moving upwards at the rate of 20~30 cm/sec. as shown in Photo. 1 where some selected frames of the film were reproduced.

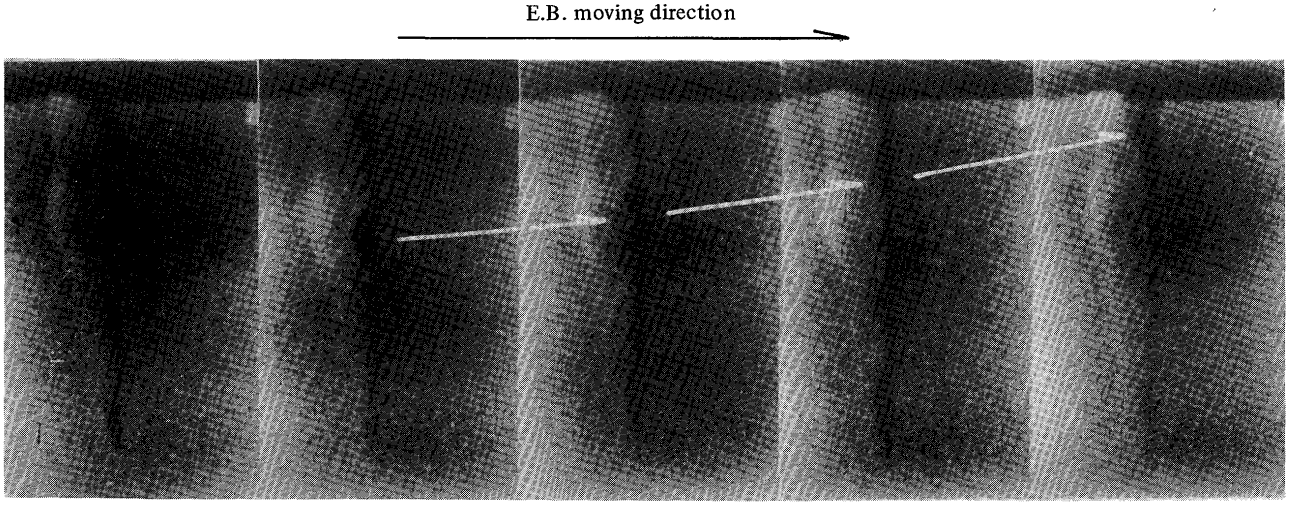


Photo. 1 Upward movement of the "wall-caves" and "wall-knobs"

At the tip of the wall-knob, the beam hole was narrowed by the dinanric force of molten fluid on the back side. But the complete closure[5] of the beam hole could not be recognized upon all these films excepting what occured at the bottom of the hole. It was difficult to estimate the wall-oscillation frequency, because the mode of fluctuation was seemed different at each part of the beam hole and the sharpened bottom of the hole was less discernable. However, the frequency was considered to be about 5 cycles/sec. in view of the movement of the wall-caves. It is different from the "natural frequency of equilibrium state" mentioned by Funk et al.[2]. This frequency was comparable to that of the spiking which was revealed by means of etching the longitudinal section of specimen after welding as illustrated in Photo. 2.

So far as this experiment was concerned, the basic fluctuation mode of the beam hole was the same for both butt-and bead-on-plate welding.

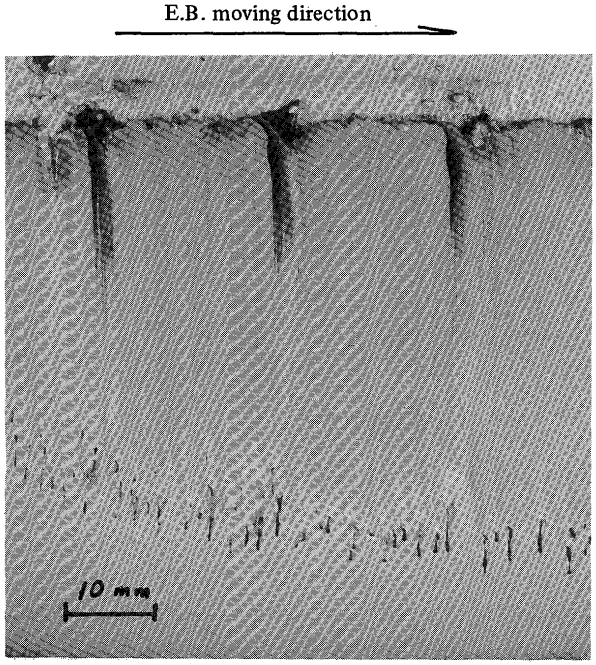


Photo. 2 Macrograph of the spiking
(Longitudinal section after welding)

### 3.4 Arched curvature of the beam hole and formation of root porosity

In most cases an arched curvature deflected in a direction opposite to that of moving was observed at the bottom side of the beam hole as shown in Photo. 3. The reson for this event is yet unknown. But it is considered that this is due to inertia, and in all liklihood it is closely related to the "wall focusing" effect[3),4)] or the "gas focusing" effect[5),6),12)] of electron beam which produces the local delay of energy assumption against the welding progression.

This event is also supposed to be concerned with the formation of root porosity. When the inflection point of the curvature is put upon a narrow part at the tip of the knob, a complete closure of the hole is easy to happen at the point. Near the bottom of beam hole, the cooling rate of molten metal is increased due to less input beam energy and becomes sufficiently rapid, and the molten metal may freeze before the trapped gas bubbles can be convected to the out side, thus giving rise to porosity in the root of weld.

### 3.5 Movement of the molten metal

The movement of molten fluid suggested by the inserted tracers of silver brazing alloy was as follows. The flow of molten metal had a very rapid rate of more than 9 m/min. in the vertical direction.

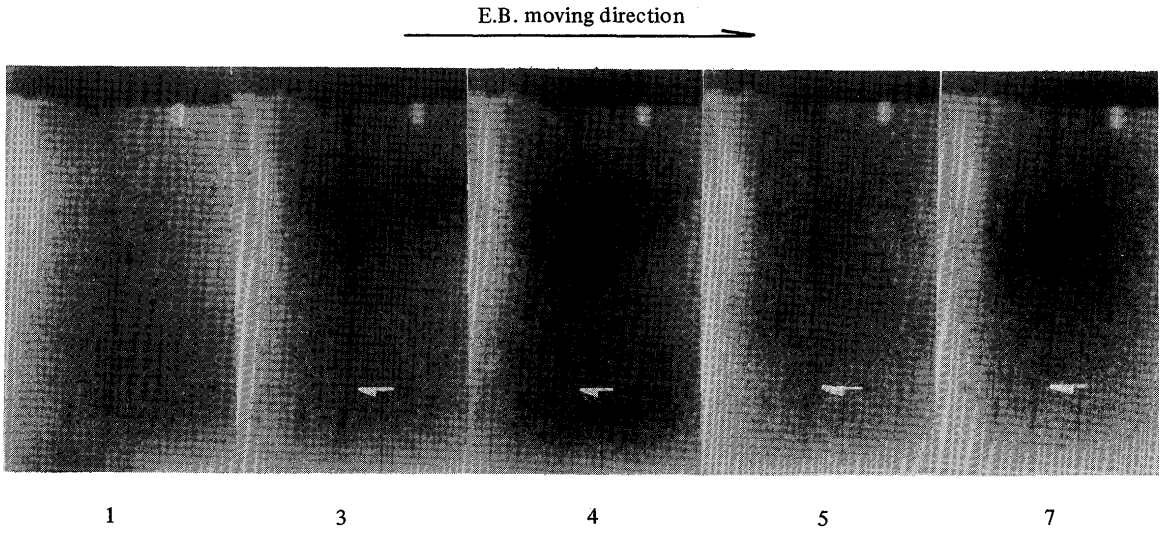


Photo. 3 Arched curvature of the beam hole and the formation of root porosity

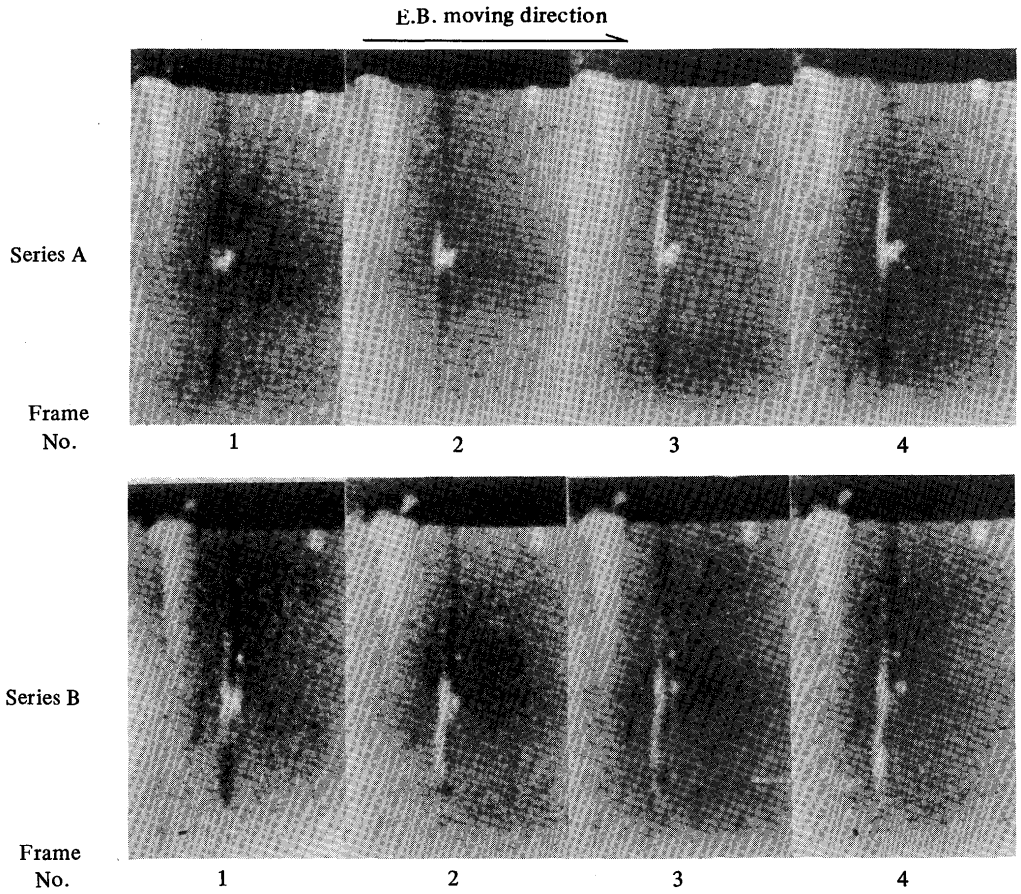


Photo. 4 Flow of the molten metal tracer (1) –middle part–

It was, of cource, recogninzed that the tracer was also spread to the rear wall through the horizontal direction[7] which was perpendicular for the X-ray passage. The details of this movement could not be clarified because the diameter of beam hole was very small.

At the middle part of the beam hole, there observed two ways of the movement. One was that the molten metal tracer contained in the fluid was at first risen up along the wall of beam hole, and about 0.1 second later, it begun to fall down towards the bottom, and finally, it was distributed through out the beam hole to be rather a symmetric appearance. In this case, the beam hole had a sharp edge at the bottom as shown in Photo. 4 series A. The other was that the tracer spread up-and downwards at the beginning, but the upward motion was less than the former and ceased after about 0.06 sec. while the downward motion continued 0.12 sec.. The final distribution was inclined towards the obtuse bottom of the

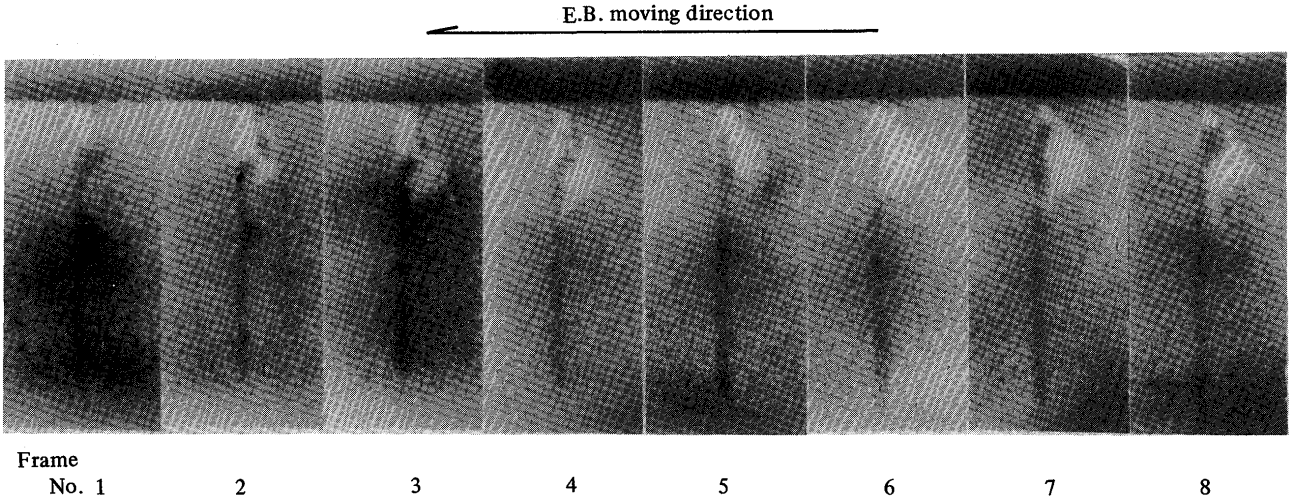


Photo. 5 Flow of the molten metal tracer (2) –upper part–

hole as shown in Photo. 4 series B..

Near the surface, the fluid moved most likely in a whirling fashion, and this event was expected to have a relation with the wave of melt reflected at the weld pool. But the attempt to observe the wave simultaneously with the hole shape was unsuccessful because the heat deposition at the surface could not make a normal bead as a result of the limitation by the employed shape of specimen head. (Photo. 5)

Although it should be noted that the difference of the specific gravity between the tracer and the base metal might disturb the natural behaviours, those turbulance in the beam hole would be very efficient for mixing the melt and resulted in a homogeneous fusion zone.

### 3.6 Formation of spiking and the influence of highly volatile elements on it.

The spiking was revealed to have an intimate relation to the instantaneous shape of beam hole. The sequence of this phenomena was as illustrated in Photo. 6 and could be explained as follows.

When the beam hole is first constricted at the upper part, underlying wall-caves of gas bubbles increase their pressure. Then at the second stage, an explosion occurs which results in breaking the balance of surroundings. Successively the back pressure of the explosion excludes the melt at the bottom of beam hole and the electron beam impingement on the dry bottom produces an additional penetration. Finally, the increase of hydrostatic head pressure makes the melt return downwards to the bottom, and the state of near equilibrium recovers again in which, for a brief instant, the back presssure of evaporation is in delicate balance with the forces of surface tension of the beam hole and the hydrostatic head of the molten pool, etc.. Metallurgical investigations of reference (10) which confirms the lack of molten metal at the root of spikes support this argument, although the movement of melt at the bottom of beam hole can not be observed in these films.

Tong and Giedt[1] proposed a model of the penetration mechanism which is a step in this direction and asserted that the formation of spiking is due to the periodic closure of beam hole by the molten metal. On the other hand, some investigators[6),8),9)] hold that the fluctuation of the energy density of electron beam caused by the collision of electrons with ionized metal vapor results in the irregular penetration which involves the spiking.

The results of our observation provide grounds for maintaining that the spiking can be formed without

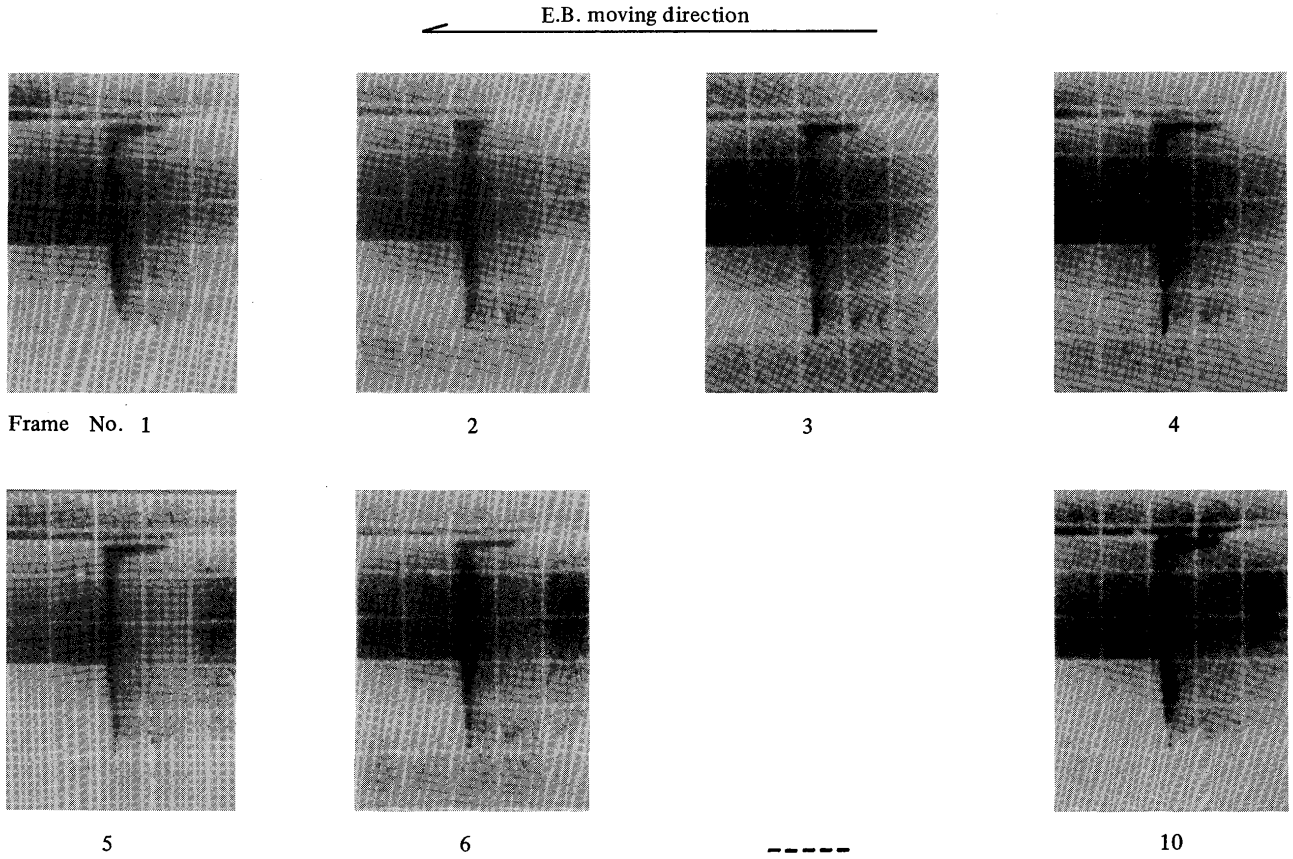


Photo. 6 Formation of spiking (from welding run No. 4)
Note: Time interval of each frame is 0.02sec

assuming the existence of such complete closure events as proposed by Tong and Giedt. In accordance with what has been stated above, the main factors which have great influence on the spiking are the pressure of metal vapor and the overhanging behaviour of molten metal. Namely occurring of the wall-caves and wall-knobs in the beam hole gives rise to spiking. It can be esily considered that the breaking of the delicate balance between these factors is not necessary to have a precise periodicity because the fluctuation of energy density of electron beam is suspected to be not directly due to the ripples of power input which shows generally a higher frequency[3),11)] than that of the spiking macrographically observed. Consequently, if the beam hole has a sort of shape which is easy to keep the balance, there appears a possibility of suppressing the spiking.

In practice, when the foils of some alloys containing a highly volatile element were inserted at the upper part of the specimen as illustrated in Fig. 3-b the spiking decreased as shown in Photo. 7.

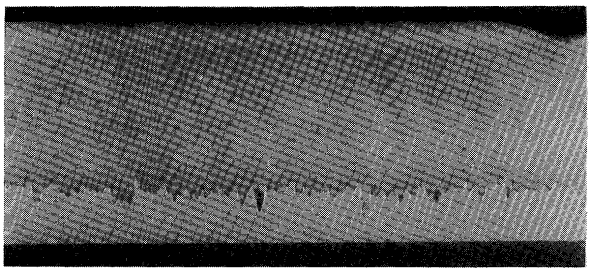

(a) Copper foil is inserted at the upper part

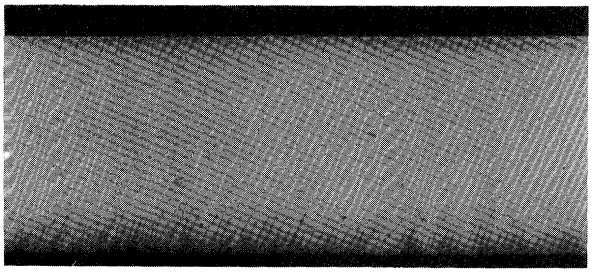

(b) Brass foil is inserted at the upper part

Photo. 7 Radiographs of aluminum specimen after welding

In this case, the beam hole became to swelled out being constiricted at the upper opening (Photo. 8) because of the increased vapor pressure, and the wall-fluctuation got to be small, while hydrostatic head increased with the growth of overhanging melt. Since the abrupt change of vapor pressure is difficult to happen under such condition, the beam hole is rather stable and the energy density in the bottom decreases because the electrons pass through the beam hole filled with dense metallic vapor. That is the most likely cause of the decrease of spiking.

E.B. moving direction

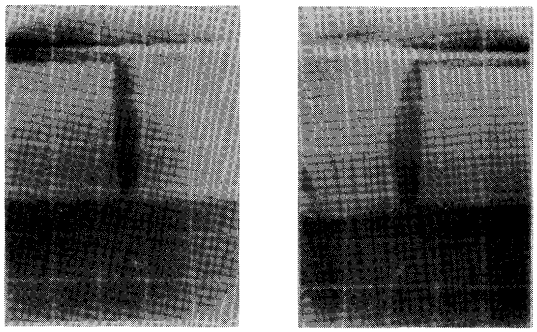

(a) A1100-(Brass) (b) 5083-(Brass)

Photo. 8 Shape of beam hole –(I)–
When brass foils are inserted at the upper part of specimens

However, when the alloy foils were inserted at the bottom side of the specimen, it was found that the influence of these foils upon the hole shape and the spiking was different with the kind of parent metal employed as the specimen. The specimens of pure aluminum eliminate the effect of inserted foils and the spiking formed again, although the specimens of 5083 alloy remained the effect.

E.B. moving direction

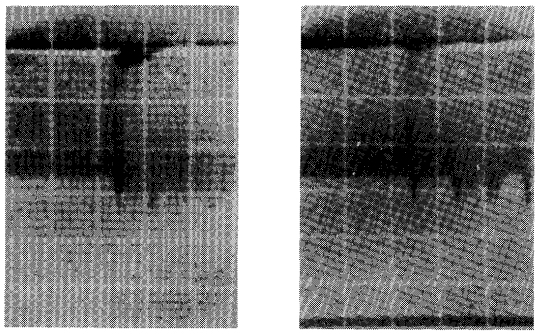

(a) A1100-(Copper) (b) A1100-(Brass)

Photo. 9 Shape of beam hole –(II)–
When copper or brass foil is inserted at the bottom side of pure aluminum

In the case of pure aluminum the surface opening of beam hole was wide. The reason for the widening is suspected to be the larger molten pool due to the transfer of less heat in the layer close to the surface. As a result of this, the metal vapor vents itself easily through the opening and the inner expansion of bem hole does not occur. Consequently the beam hole becomes narrow at the middle and lower part where the constriction of the hole and the explosion of gas babbles occur to form the spiking.

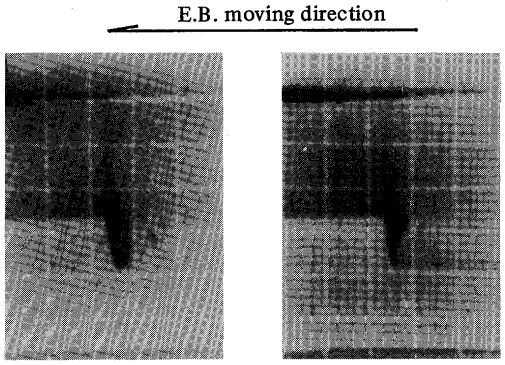


(a) 5083-(Brass) (b) 5083-(Phosphor bronze)

Photo. 10 Shape of beam hole –(III)–
When brass or phosphor bronze foil is inserted at the bottom side of 5083 alloy

On the other hand, the passage in 5083 alloy was constricted and narrowed between the opening and the upper end of inserted foil as shown in Photo. 10, because of heat dissipation by the intense evaporation of magnesium contained in the alloy. As the expansion of beam hole still remained at the bottom side, the spike decreasing effect was not disappeared.

## 4. Summary

A cine-fluoroscopic technique has been developed for studying the dynamic mechanism of electron beam welding using aluminum alloys. Although further experiments are necessary to clarify the mechanism more precisely, because a different phenomenon may be observed in the specimens of steels, etc., the following conclusions are possible from the evidence obtained in this experiment.

(1) By means of the technique combined with metal tracers, a direct observation of the beam hole and in part the molten metal during electron beam welding can be achieved with a fairly excellent resolution on the movie film.

(2) The beam hole generally does not hold a steady shape and oscillates in width and depth. The strong wall-fluctuation occurs so frequent and it gives rise to the wall-caves and wall-knobs. They move upward at the rapid rate of 20–30 cm/sec, for example.

(3) The higher welding speed becomes the more the beam hole bends like an arch convexed toward the direction of welding progression. This event has a considerable effect on the formation of root porosity.

(4) The formation of spiking is resulted from the breakdown of the balance between the vapor pressure and the hydrostatic head of the melt and in addition dynamic force of the molten fluid, and is revealed to have an intimate relation with occurring of the wall-caves and wall-knobs in the beam hole. It can be suppressed when the stable beam hole is produced by inserting the alloy foils which containes a highly volatile element.

(5) The molten metal flows up and down along the wall of beam hole at quite a high travel rate. That accounts for the favourable homogeneity of fusion zone caused by metal mixing.

### References

1) H. Tong and W. H. Giedt: A Dynamic Interpretation of Electron Beam Welding, W. J. 49-6 (1970), 259s.
2) E. R. Funk, R.C. McMaster et al.: Penetration Mechanisms of Electron Beam Welding and the Spiking Phenomenon, W. J. 53-6 (1974), 246s.
3) Y. Arata et al. : Energy Distribution in the Hole of Electron Beam Welding, Report of EBW Research Committee of JWS (1975), EBW-123-75, (in Japanese)
4) Y. Arata and I. Miyamoto; Processing Mechanism of High Energy Density Beam (Rept. 1) –Mechanism of Drilling–, Trans. of TWRI, Vol. 2, No. 2 (1973) 19
5) H. Schwarz: Present Knowledge of the F oundamental Processes of Electron Beam As a Material Working Tools, The 3rd Inter. Conf. on Electron and Ion Beam Science and Technology (1968), 301
6) V. P. Ledovskoy et al.: Plasma-Beam Interaction during Electron Beam welding, IEE Conf. Publ. (Inst. Electr. Eng.) (1974), 563
7) N. A. Ol'shanskii et al.: Movement of Molten Metal during Electron Beam Weldong, Svar. Proiz. 21-9, (1974), 12
8) R. E. Armstrong: Spiking in Partial Penetration Electron Beam Welds, The 4th Intern. Conf. on Electron and Ion Beam Science and Technoloty (1970), 179.
9) G. K. Hicken and W. G. Booco: Penetration Variations in Electron Beam Welding, The 3rd Intern. Conf. on Electron and Ion Beam Science and Technology, (1968), 398.
10) Y. Arata, S. Matsuda et al. Study on Characteristics of Weld Defect and Its Prevention in Electron Beam Welding (Report III), Trans. of JWRI, 3-2, (1974), 81.
11) V. I. Leskov et al.: Mechanism in Deep Weld Pools During Electron-Beam Welding, Avt. Svarka. 28-1, (1975), 12
12) J. W. Meier: Electron Beam Welding Characteristics of Several Materials, Proc. 3rd Symp. on EB Tech., (1961), 145